Astronomy & Astrophysics manuscript no. H2CS-isos_11
December 1, 2018

Laboratory spectroscopic study of isotopic thioformaldehyde, H_2CS, and determination of its equilibrium structure⋆

Holger S. P. Müller[1], Atsuko Maeda[2], Sven Thorwirth[1], Frank Lewen[1], Stephan Schlemmer[1], Ivan R. Medvedev[2,⋆⋆], Manfred Winnewisser[2], Frank C. De Lucia[2], and Eric Herbst[2,⋆⋆⋆]

[1] I. Physikalisches Institut, Universität zu Köln, Zülpicher Str. 77, 50937 Köln, Germany
e-mail: hspm@ph1.uni-koeln.de
[2] Department of Physics, The Ohio State University, Columbus, OH 43210-1107, USA

Received 26 October 2018 / Accepted 22 November 2018

ABSTRACT

Context. Thioformaldehyde is an abundant molecule in various regions of the interstellar medium. However, available laboratory data limit the accuracies of calculated transition frequencies in the submillimeter region, in particular for minor isotopic species.
Aims. We aim to determine spectroscopic parameters of isotopologs of H_2CS that are accurate enough for predictions well into the submillimeter region.
Methods. We investigated the laboratory rotational spectra of numerous isotopic species in natural isotopic composition almost continuously between 110 and 377 GHz. Individual lines were studied for most species in two frequency regions between 566 and 930 GHz. Further data were obtained for the three most abundant species in the 1290−1390 GHz region.
Results. New or improved spectroscopic parameters were determined for seven isotopic species. Quantum-chemical calculations were carried out to evaluate the differences between ground state and equilibrium rotational parameters to derive semi-empirical equilibrium structural parameters.
Conclusions. The spectroscopic parameters are accurate enough for predictions well above 1 THz with the exception of $H_2^{13}C^{34}S$ where the predictions should be reliable to around 700 GHz.

Key words. Molecular data – Methods: laboratory: molecular – Techniques: spectroscopic – Radio lines: ISM – ISM: molecules – Astrochemistry

1. Introduction

Thioformaldehyde, H_2CS, was among the molecules detected early in space, namely in the giant high-mass starforming region Sagittarius B2 near the Galactic center (Sinclair et al. 1973). The molecule was also detected in dark clouds, such as TMC-1 and L134N (Irvine et al. 1989), and in the circumstellar envelope of the C-rich asymptotic giant branch (AGB) star CW Leonis, also known as IRC +10216 (Agúndez et al. 2008). Concerning solar system objects, H_2CS was detected in the comet Hale Bopp (Woodney et al. 1997). Furthermore, it was detected in nearby galaxies, such as the Large Magellanic Cloud (Heikkilä et al. 1999) and NGC253 (Martín et al. 2005), and also in more distant galaxies, such as the $z = 0.89$ foreground galaxy in the direction of the blazar PKS 1830−211 (Muller et al. 2011). Several isotopic species were detected as well; $H_2C^{34}S$ (Gardner et al. 1985), $H_2^{13}CS$ (Cummins et al. 1986), HDCS (Minowa et al. 1997), and even D_2CS (Marcelino et al. 2005); unlabeled atoms refer to ^{12}C and ^{32}S.

Spectroscopic identifications of thioformaldehyde were based on molecular parameters which were obtained to a large extent from laboratory rotational spectroscopy. The first results were reported by Johnson & Powell (1970) followed by additional measurements of H_2CS and, to a much lesser extent, of $H_2C^{34}S$, $H_2^{13}CS$, and D_2CS up to 70 GHz (Johnson et al. 1971). Beers et al. (1972) measured further transitions of H_2CS up to 244 GHz. Cox et al. (1982) carried out microwave measurements of several minor thioformaldehyde isotopologs and determined dipole moments for H_2CS and D_2CS; a very accurate H_2CS dipole moment was reported by Fabricant et al. (1977). Brown et al. (1987) investigated the ^{33}S and ^{13}C hyperfine structure (HFS) from microwave transitions. Minowa et al. (1997) determined HDCS transition frequencies from the millimeter to the lower submillimeter regions. Additional, though less accurate data for H_2CS and $H_2C^{34}S$ were obtained in a far-infrared study of thioformaldehyde (McNaughton & Bruget 1993) and from the A−X electronic spectrum of H_2CS (Clouthier et al. 1994). Further, quite accurate transition frequencies of HDCS and D_2CS were obtained from radio-astronomical observations (Marcelino et al. 2005).

The need for higher frequency data was apparent in molecular line surveys of Orion KL carried out with the Caltech Submillimeter Observatory (CSO) on Mauna Kea, Hawaii covering 325−360 GHz (Schilke et al. 1997) and 607−725 GHz (Schilke

⋆ Transition frequencies from this work as well as related data from earlier work are given for each isotopic species as supplementary material. Given are also quantum numbers, uncertainties, and residuals between measured frequencies and those calculated from the final sets of spectroscopic parameters. The data are available at CDS via anonymous ftp to cdsarc.u-strasbg.fr (130.79.128.5) or via http://cdsweb.u-strasbg.fr/cgi-bin/qcat?J/A+A/

⋆⋆ Current address: Department of Physics, Wright State University, Dayton, OH 45435 USA.
⋆⋆⋆ Current address: Departments of Chemistry and Astronomy, University of Virginia, Charlottesville, VA 22904, USA.

Article published by EDP Sciences, to be cited as https://doi.org/10.1051/0004-6361/201834517

et al. 2001), and those carried out with the *Odin* satellite covering 486−492 GHz and 541−577 GHz (Olofsson et al. 2007; Persson et al. 2007), the one carried out with the *Herschel* satellite covering 480−1280 GHz and 1426−1907 GHz (Crockett et al. 2014), and the the *Herschel* molecular line survey of Sagittarius B2(N) (Neill et al. 2014). Moreover, the identification of $H_2C^{34}S$ in the Protostellar Interferometric Line Survey (PILS) of IRAS 16293−2422 with the Atacama Large Millimeter/submillimeter Array (ALMA) between 329 and 363 GHz (Drozdovskaya et al. 2018) may have been hampered by insufficient accuracies of some of the rotational transitions.

The apparent lack of accuracy in the H_2CS rest-frequencies in the higher frequency CSO survey (Schilke et al. 2001) and a specific request from a member of the *Odin* team to one of us (E.H.) initiated our study covering 110−377 GHz, 566−670 GHz, and 848−930 GHz. An account on the H_2CS data in the ground vibrational state has been given by Maeda et al. (2008). Later, we extended measurements to the 1290−1390 GHz region. Here, we report on the ground state rotational data of seven isotopic species, H_2CS, $H_2C^{33}S$, $H_2C^{34}S$, $H_2C^{36}S$, $H_2^{13}CS$, $H_2^{13}C^{34}S$, and HDCS obtained from samples in natural isotopic composition. The derived, often greatly improved, spectroscopic parameters permit predictions of accurate rest-frequencies well above 1 THz except for $H_2^{13}C^{34}S$, where the experimental data are more limited. The rotational parameters of these isotopologs plus a set of redetermined values for D_2CS combined with vibration-rotation parameters from quantum-chemical calculations were used to derive equilibrium structural parameters.

2. Laboratory spectroscopic details

We employed the Fast Scan Submillimeter-wave Spectroscopic Technique (FASSST) of The Ohio State University (OSU) to cover the 110−377 GHz range with a small gap at 190−200 GHz (Petkie et al. 1997; Medvedev et al. 2004). Additionally, we used two different spectrometer systems at the Universität zu Köln to record higher frequency transitions up to almost 1.4 THz (Winnewisser et al. 1994; Winnewisser 1995; Xu et al. 2012).

The FASSST system employs backward wave oscillators (BWOs) as sources; in the present study one that covered about 110−190 GHz and two spanning the region of 200−377 GHz. The frequency of each BWO was swept quickly so that a wide frequency range (∼90 GHz) can be measured in a short period and any voltage instability of the BWOs can be overcome. The frequency of the FASSST spectrum was calibrated with sulfur dioxide (SO_2) rotational lines whose spectral frequencies are well known (Müller & Brünken 2005). A portion of the source radiation propagated through a Fabry-Perot cavity to produce an interference fringe spectrum with a free spectral range of ∼9.2 MHz. The frequencies of radiation between the calibration lines were interpolated with the fringe spectrum. In the calibration procedure, the dispersive effect of atmospheric water vapor in the Fabry-Perot cavity was taken into account (Maeda et al. 2006; Groner et al. 2007). Measurements were taken with scans that proceeded both upward and downward in frequency so as to record an average frequency. The results obtained from 100 upward and downward scans were accumulated for a better signal-to-noise ratio, increasing the integration time from ∼0.1 to ∼10 ms. The experimental uncertainty of this apparatus is around 50 kHz for an isolated, well-calibrated line.

We used phase-lock loop (PLL) systems in the Cologne spectrometers to obtain accurate frequencies. Two BWOs were used as sources to record lines in the 566−670 and 848−930 GHz regions. A portion of the radiation from the BWOs was mixed with an appropriate harmonic of a continuously tunable synthesizer in a Schottky diode multiplier mixer to produce the intermediate frequency (IF) signal. The IF-signal was phase-locked and phase-error provided by the PLL circuit were fed back to the power supply of the BWOs. The experimental uncertainties under normal absorption conditions can be as low as 5 kHz even around 1 THz (Belov et al. 1995; Müller et al. 2007).

A solid-state based spectrometer system was used to obtain transition frequencies between 1290 and 1390 GHz. A set of frequency multipliers (three doublers plus two triplers) were driven by a microwave synthesizer to cover these frequencies. Additional detail is given by Xu et al. (2012). Accuracies of 10 kHz can be achieved for strong, isolated lines (Müller et al. 2015; Müller & Lewen 2017).

Thioformaldehyde (H_2CS) was produced by the pyrolysis of trimethylene sulfide [$(CH_2)_3S$; Sigma-Aldrich Co.], which was used as provided. The thermal decomposition of trimethylene sulfide yields mostly thioformaldehyde and ethylene, which has no permanent dipole moment, but also small amounts of by-products such as CS, H_2S, and H_2CCS. Laboratory setups for the pyrolysis were slightly different in the OSU and Cologne measurements. At OSU, trimethylene sulfide vapor was passed through a 2 cm diameter, 20 cm long piece of quartz tubing stuffed with quartz pieces and quartz cotton to enlarge the reaction surface. The quartz tubing was heated with a cylindrical furnace to ∼680°C. The gas produced from the pyrolysis was introduced to a 6 m long aluminum cell at room temperature and pumped to a pressure of 0.4−1.5 mTorr (1 mTorr = 0.1333 Pa). The spectrum of trimethylene sulfide almost totally disappeared after the pyrolysis, at which time the spectrum of thioformaldehyde appeared. Spectral lines due to the by-products, CS, H_2S, and H_2CCS, were also observed, but with less intensity compared with thioformaldehyde.

A 3 m long glass absorption cell kept at room temperature was used for measurements in Cologne. A higher temperature of about 1300°C was required in the pyrolysis zone in order to maximize the thioformaldehyde yield and to minimize absorptions of $(CH_2)_3S$ because no quartz cotton was used in the quartz pyrolysis tube. The total pressure was around 1−3 Pa for weaker lines and around 0.01−0.1 Pa for stronger lines.

Liquid He-cooled InSb bolometers were used in both laboratories as detectors.

3. Quantum-chemical calculations

Hybrid density functional calculations of the B3LYP variant (Becke 1993; Lee et al. 1988) and Møller-Plesset second order perturbation theory (MP2) calculations (Møller & Plesset 1934) were carried out with the commercially available program Gaussian 09 (Frisch et al. 2013). We performed also coupled cluster calculations with singles and doubles excitations augmented by a perturbative correction for triple excitations, CCSD(T) (Raghavachari et al. 1989) with the 2005 Mainz-Austin-Budapest version of ACESII and its successor CFOUR[1]. We employed correlation consistent basis sets cc-pVXZ (X = T, Q, 5) (Dunning 1989) for H and C and the cc-pV(X+d)Z basis sets for S (Dunning et al. 2001); diffuse basis functions were augmented for some calculations, denoted as aug-cc-pVXZ and aug-cc-pV(X+d)Z. We abbreviate these basis sets as XZ and aXZ, re-

[1] CFOUR, a quantum chemical program package written by J. F. Stanton, J. Gauss, M. E. Harding, P. G. Szalay et al. For the current version, see http://www.cfour.de

spectively. In addition, we employed weighted core-correlating basis functions in some cases, yielding the (aug-) cc-pwCVXZ basis sets (Peterson & Dunning 2002). These basis sets were abbreviated as wCXZ and awCXZ, respectively. All calculation were carried aut at the Regionales Rechenzentrum der Universität zu Köln (RRZK).

Equilibrium geometries were determined by analytic gradient techniques, harmonic force fields by analytic second derivatives, and anharmonic force fields by numerical differentiation of the analytically evaluated second derivatives of the energy. The main goal of these anharmonic force field calculations was to evaluate first order vibration-rotation parameters (Mills 1972), see also Sect. 6. Core electrons were kept frozen in MP2 and CCSD(T) calculations unless "ae" indicates that all electrons were correlated. We evaluated the hyperfine parameters of $H_2C^{33}S$ using the awCQZ basis set (wCQZ for CCSD(T) calculation) at the equilibrium geometry calculated at the same level.

4. Spectroscopic properties of thioformaldehyde

Thioformaldehyde is an asymmetric rotor with $\kappa = (2B - A - C)/(A - C) = -0.9924$, much closer to the symmetric limit of -1 than the isovalent formaldehyde for which κ is -0.9610, see, for example, Müller & Lewen (2017). The H_2CS dipole moment of 1.6491 D (Fabricant et al. 1977) is aligned with the a inertial axis. The strong rotational transitions are therefore those with $\Delta K_a = 0$ and $\Delta J = +1$, that is, the R-branch transitions. Transitions with $\Delta K_a = 0$ and $\Delta J = 0$ (Q-branch transitions) are also allowed as are transitions with $\Delta K_a = \pm 2$. These transitions are not only much weaker than the strong R-branch transitions, but also relatively weaker than the equivalent transitions in H_2CO because H_2CS is closer to the symmetric prolate limit.

Isotopologs with two H or two D have C_{2v} symmetry whereas isotopologs with one H and one D have C_S symmetry. Spin-statistics caused by the two equivalent H lead to *ortho* and *para* states with a 3 : 1 intensity ratio. The *ortho* states are described by K_a being odd. The *ortho* to *para* ratio in D_2CS is 2 : 1, and the *ortho* states are described by K_a being even. No non-trivial spin-statistics exist in HDCS and related isotopologs.

Sulfur has four stable isotopes with mass numbers 32, 33, 34, and 36 and with terrestrial abundances of 95.0 %, 0.75 %, 4.2 %, and ∼0.015 %, respectively (Berglund & Wieser 2011). The respective abundances are 98.89 % and 1.11 % for ^{12}C and ^{13}C and 99.98 % and ∼0.015 % for H and D.

5. Spectroscopic results

We used Pickett's SPCAT and SPFIT programs (Pickett 1991) to predict and fit rotational spectra of the various isotopic species of thioformaldehyde. Predictions were generated from the published data for the isotopic species H_2CS, $H_2C^{34}S$, $H_2C^{33}S$, $H_2^{13}CS$, and HDCS (Johnson et al. 1971; Beers et al. 1972; Cox et al. 1982; Brown et al. 1987; McNaughton & Bruget 1993; Minowa et al. 1997). Higher order spectroscopic parameters of isotopic species with heavy atom substition were estimated from those of H_2CS by scaling the parameters with appropriate powers of the ratios of $2A - B - C$, $B + C$, and $B - C$. Even though these estimates do not hold strictly, they are almost always better than constraining the parameters to zero and also mostly better than contraining the parameters to values directly taken from the main isotopic species, see, e.g., below or the examples of isotopic CH_3CN (Müller et al. 2016) or H_2CO (Müller & Lewen 2017). This scaling procedure is not recommended for H to D substitution especially in molecules with relatively few atoms, such as HDCS. The resulting spectroscopic line lists are or were available in the Cologne Database for Molecular Spectroscopy, CDMS[2] (Endres et al. 2016) as version 1, mostly from February 2006. An updated entry (version 2) has been available for the H_2CS main isotopic species since early 2008.

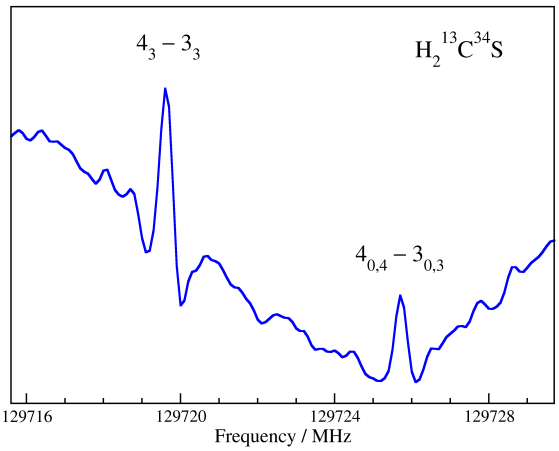

Fig. 1. Section of the rotational spectrum of $H_2^{13}C^{34}S$ recorded in natural isotopic composition, showing two low-J lines. K_c was omitted for the $K_a = 3$ transitions because the asymmetry splitting was not resolved and $K_c = J - K_a$ or $K_c = J - K_a + 1$.

We carried out the rotational assignment for the FASSST spectra of thioformaldehyde with the Computer Aided Assignment of Asymmetric Rotor Spectra (CAAARS) program applying the Loomis-Wood procedure, with which the observed spectrum is visually compared with predicted line positions and intensities to make new assignments (Medvedev et al. 2005). The strong $\Delta K_a = 0$ R-branch transitions of the abundant isotopic species H_2CS, $H_2C^{34}S$, $H_2^{13}CS$, and $H_2C^{33}S$ were found easily first for low values of K_a (0–4) and later up to $K_a = 9$. The upper frequency of 377 GHz limited the J quantum numbers to a maximum of $10 - 9$ for H_2CS and $11 - 10$ for the other isotopologs because of the smaller values of $B + C$. Several transitions of $H_2C^{33}S$ displayed splitting caused by the electric nuclear quadrupole moment and the magnetic nuclear dipole moment of the $I = 3/2$ nucleus of ^{33}S. We could also make extensive assignments for the weaker Q-branch transitions with $K_a = 1$. These covered all and almost all of $J = 15$ to 26 for H_2CS and $H_2C^{34}S$, respectively; fewer lines were found for $H_2^{13}CS$ and $H_2C^{33}S$. In the case of the main isotopic species, we could assign most of the even weaker $K_a = 2$ Q-branch transitions with $32 \le J \le 41$.

On the basis of these extensive assignments, we suspected that transitions of HDCS should be strong enough in natural isotopic composition to identify them in our FASSST spectra. Minowa et al. (1997) had reported transition frequencies from laboratory measurements up to 380 GHz. The resulting spectroscopic parameters were sufficiently accurate to identify HDCS transitions in our FASSST spectra. Even though the lines were weak, we could supplement the existing line list with R-branch transition frequencies not reported by Minowa et al. (1997) up to $K_a = 7$.

With the identification of HDCS in the FASSST spectra, it appeared plausible to search for transitions of $H_2^{13}C^{34}S$ and $H_2C^{36}S$ because they have abundances similar to those of HDCS. We derived an $r_{I,\epsilon}$ structure (Rudolph 1991), see also Sect. 6,

[2] http://www.astro.uni-koeln.de/cdms/entries

Table 1. Spectroscopic parameters[a,b] (MHz) of thioformaldehyde isotopologs with different sulfur isotopes.

Parameter	H_2CS	$H_2C^{33}S$	$H_2C^{34}S$	$H_2C^{36}S$
$A-(B+C)/2$	274437.5932 (115)	274588.054 (306)	274729.12 (34)	274987.91 (94)
$(B+C)/2$	17175.745955 (196)	17024.740821 (110)	16882.911552 (112)	16621.73726 (35)
$(B-C)/4$	261.6240523 (165)	257.050936 (39)	252.793027 (73)	245.04552 (43)
D_K	23.34378 (164)	23.408	23.468 (141)	23.6
D_{JK}	0.5222938 (43)	0.5132638 (95)	0.5048431 (51)	0.489486 (38)
$D_J \times 10^3$	19.01875 (39)	18.700456 (105)	18.404173 (172)	17.86334 (29)
$d_1 \times 10^3$	−1.208429 (105)	−1.176656 (78)	−1.148425 (108)	−1.09806 (36)
$d_2 \times 10^3$	−0.1773270 (222)	−0.171180 (81)	−0.165589 (136)	−0.15585 (27)
$H_K \times 10^3$	5.946 (35)	5.97	6.00	6.05
$H_{KJ} \times 10^6$	−28.155 (86)	−27.839 (211)	−28.071 (109)	−28.16 (61)
$H_{JK} \times 10^6$	1.50409 (270)	1.4502 (39)	1.41629 (70)	1.3346 (203)
$H_J \times 10^9$	−5.81 (32)	−5.46	−5.100 (40)	−4.48
$h_1 \times 10^9$	3.018 (141)	2.792	2.600 (37)	2.216
$h_2 \times 10^9$	1.6472 (140)	1.524	1.415 (49)	1.209
$h_3 \times 10^9$	0.3619 (73)	0.3393	0.3186 (144)	0.2796
$L_K \times 10^6$	−2.109 (206)	−2.00	−2.00	−2.00
$L_{KKJ} \times 10^9$	−21.36 (69)	−23.18 (128)	−20.86 (65)	−20.37
$L_{JK} \times 10^9$	0.2032 (90)	0.200	0.197	0.1909
$L_{JJK} \times 10^{12}$	−10.32 (81)	−9.66	−9.0	−7.85
$L_J \times 10^{12}$	0.833 (87)	0.766	0.700	0.588
$l_1 \times 10^{12}$	−0.358 (47)	−0.330	−0.304	−0.258
$P_{KKJ} \times 10^{12}$	−18.63 (180)	−18.8	−19.0	−19.0

Notes. [(a)] Watson's S reduction has been used in the representation I^r. Numbers in parentheses are one standard deviation in units of the least significant figures. Parameters without uncertainties were estimated and kept fixed in the analyses. [(b)] ^{33}S HFS parameters are given in Table 2.

Table 2. Experimental ^{33}S hyperfine structure parameters[a] (MHz) of $H_2C^{33}S$ in comparison to equilibrium values from quantum-chemical calculations[b].

Parameter	exptl.	B3LYP	MP2	ae-MP2	ae-CCSD(T)
χ_{aa}	−11.8893 (124)	−12.27	−10.31	−9.99	−12.818
χ_{bb}	49.9668 (156)	50.26	49.08	48.93	50.030
χ_{cc}[c]	−38.0775 (158)	−37.99	−38.77	−38.94	−37.212
$(C_{aa}-(C_{bb}+C_{cc})/2) \times 10^3$	475.5 (24)	526.5	469.3	468.5	456.0
$(C_{bb}+C_{cc}) \times 10^3$	13.6	15.28	13.61	13.63	13.6
$(C_{bb}-C_{cc}) \times 10^3$	10.68 (105)	10.98	10.29	10.33	10.2

Notes. [(a)] Numbers in parentheses are one standard deviation in units of the least significant figures. Parameters without uncertainties were estimated and kept fixed in the analyses. [(b)] Basis sets: aug-cc-pwCVQZ for B3LYP and MP2 calculations, cc-pwCVQZ for ae-CCSD(T); see also section 3. [(c)] Derived value because the sum of the χ_{ii} is zero.

from the known rotational parameters because this structure model can provide good predictions of rotational parameters of isotopologs not yet studied, see, e.g., the example of cyclopropylgermane (Epple & Rudolph 1992) or sulfuryl chloride fluoride (Müller & Gerry 1994). We were able to make assignments of R-branch transition up to $K_a = 5$ for both isotopic species, however, those for $H_2^{13}C^{34}S$ were only made in the process of writing this manuscript, and assignments extend only up to 362 GHz.

Most of the frequencies were assigned uncertainties of 50 kHz; 100 kHz were assigned to the weak Q-branch transition frequencies, to some of the weaker $H_2C^{33}S$ lines, and to the stronger $H_2C^{36}S$ lines. Uncertainties of 200 kHz were assigned to weaker lines of $H_2C^{36}S$.

Subsequently, improved predictions were used to search for individual transitions of H_2CS, $H_2C^{34}S$, $H_2^{13}CS$, $H_2C^{33}S$, HDCS, and $H_2C^{36}S$ in the regions 566−670 and 848−930 GHz using the Cologne Terahertz Spectrometer. Fig. 2 demonstrates the good signal-to-noise ratio achieved for HDCS. Later, we recorded transitions of H_2CS, $H_2C^{34}S$, and $H_2^{13}CS$ in the 1290−1390 GHz region. Fig. 3 demonstrates the *para* to *ortho* ratio for the main isotopic species. The Boltzmann peak of the room temperature rotational spectrum of H_2CS is at ∼800 GHz. Therefore, we did not attempt any measurements for the rarer isotopic species at these high frequencies.

The quantum numbers of the strong R-branch transitions reach $J = 41 - 40$ and $K_a = 15$ for H_2CS; we recorded three

Table 3. Spectroscopic parameters[a] (MHz) of $H_2^{13}CS$, $H_2^{13}C^{34}S$, HDCS, and D_2CS.

Parameter	$H_2^{13}CS$	$H_2^{13}C^{34}S$	HDCS	D_2CS
$A-(B+C)/2$	275113.82 (35)	275418.9 (161)	187214.14 (44)	132198.92 (26)
$(B+C)/2$	16514.989247 (141)	16219.21918 (122)	15501.179704 (242)	14200.0562 (59)
$(B-C)/4$	241.898578 (82)	233.32414 (81)	304.81583 (44)	352.105440 (153)
D_K	23.465 (129)	23.51	13.364 (198)	5.5
D_{JK}	0.4960263 (70)	0.478799 (57)	0.3208611 (107)	0.29091 (146)
$D_J \times 10^3$	17.692846 (203)	17.0998 (66)	15.40446 (68)	12.492 (158)
$d_1 \times 10^3$	−1.071785 (122)	−1.01853	−1.38941 (86)	−1.40268 (225)
$d_2 \times 10^3$	−0.152488 (113)	−0.14239	−0.23009 (42)	−0.28995 (37)
$H_K \times 10^3$	6.00	6.00	3.0	0.75
$H_{KJ} \times 10^6$	−25.846 (164)	−25.77	−37.662 (110)	−4.7
$H_{JK} \times 10^6$	1.34969 (281)	1.271	1.2332 (61)	0.88
$H_J \times 10^9$	−5.660 (45)	−4.97	1.885 (288)	1.3
$h_1 \times 10^9$	2.577 (39)	2.21	2.75 (52)	3.0
$h_2 \times 10^9$	1.292 (38)	1.11	1.92 (32)	1.719 (109)
$h_3 \times 10^9$	0.3009 (110)	0.2645	0.50	0.792 (33)
$L_K \times 10^6$	−2.00	−2.00		
$L_{KKJ} \times 10^9$	−22.16 (106)	−21.65		
$L_{JK} \times 10^9$	0.189	0.183		
$L_{JJK} \times 10^{12}$	−10.06	−8.80		
$L_J \times 10^{12}$	0.750	0.630		
$l_1 \times 10^{12}$	−0.320	−0.272		
$P_{KKJ} \times 10^{12}$	−19.0	−19.0		

Notes. [(a)] Watson's S reduction has been used in the representation I^r. Numbers in parentheses are one standard deviation in units of the least significant figures. Parameters without uncertainties were estimated and kept fixed in the analyses.

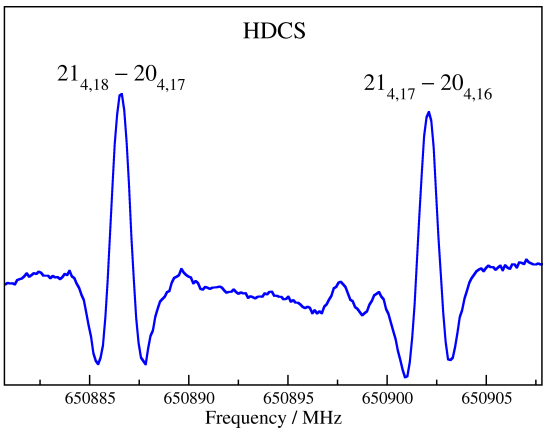

Fig. 2. Section of the rotational spectrum of HDCS recorded in natural isotopic composition, displaying the $K_a = 4$ asymmetry splitting. The identities of the weaker features are not known.

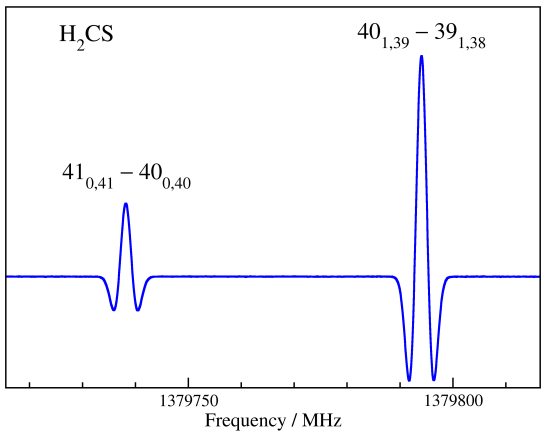

Fig. 3. Section of the rotational spectrum of H_2CS displaying the *para* to *ortho* ratio of 1 to 3.

$K_a = 1$ Q-branch transitions up to $J = 41$ and five $K_a = 2 - 0$ or $3 - 1$ P-branch transitions ($\Delta J = -1$) below 1 THz. In the case of $H_2C^{34}S$ and $H_2^{13}CS$, $J = 42 - 41$, $K_a = 12$ and $J = 43 - 42$, $K_a = 11$ were reached. In addition, we recorded two $K_a = 1$ Q-branch transitions with $J = 34$ and 35 for $H_2C^{34}S$. Finally, $J = 27 - 26$, $K_a = 11$ and $J = 28 - 27$, $K_a = 7$, and $J = 30 - 29$, $K_a = 9$ were reached for $H_2C^{33}S$, $H_2C^{36}S$, and HDCS, respectively. Unfortunately, we did not attempt to search for transitions of $H_2^{13}C^{34}S$ in the (initial) absence of assignments in the FASSST spectra.

Uncertainties of 5 kHz were assigned to the best lines of almost all isotopic species below 1 THz, 10 kHz were assigned to the best lines of $H_2C^{36}S$ and those above 1 THz. The largest uncertainties were around 50 kHz.

Our data set for the main isotopic species is very similar to that of our earlier account by Maeda et al. (2008). The main exception are 58 transitions corresponding to 42 frequencies because of unresolved asymmetry splitting at higher K_a that were recorded between 1290 and 1390 GHz. We omitted the far-infrared transition frequencies from McNaughton & Bruget

(1993) below 1390 GHz or 46.37 cm^{-1} because of the lower accuracy of these data (~3 MHz). Additional data beyond our transition frequencies are the ground state combination differences from the A−X electronic spectrum of H_2CS (Clouthier et al. 1994) and lower frequency rotational transitions frequencies (Fabricant et al. 1977; Johnson et al. 1971; Beers et al. 1972). Some transition frequencies for $H_2C^{34}S$ and $H_2^{13}CS$ were taken from Johnson et al. (1971) and from Cox et al. (1982); Brown et al. (1987) contributed data for $H_2C^{33}S$ and for $H_2^{13}CS$, and Minowa et al. (1997) for HDCS. We determined also spectroscopic parameters for D_2CS in particular for the structure determination even though we did not record any transitions of this rare isotopolog. We combined earlier laboratory data (Johnson et al. 1971; Cox et al. 1982) with more recent rest frequencies from radio astronomical observations (Marcelino et al. 2005).

The HFS components of the $2_{1,1} - 2_{1,2}$ transition of $H_2C^{33}S$ (Brown et al. 1987) displayed average residuals between measured and calculated frequencies of 28 kHz, much larger than the assigned uncertainties of 4−8 kHz and with considerable scatter. Therefore, we omitted the HFS components of this transition from the final fit.

The additional very acurate data for the main isotopic species from the 1290−1390 GHz region required two additional parameters, L_{JJK} and L_J, in the fit compared with our previous report (Maeda et al. 2008). The parameter values changed only very little for the most part with the exception of H_J, which changed from (−3.33 ± 0.29) mHz to (−5.81 ± 0.31) mHz.

Sets of spectroscopic parameters were evaluated for $H_2C^{34}S$ and $H_2^{13}CS$ as described above. Parameters derived from the main isotopic species were fit starting from the lower order parameters. A parameter was considered to be kept floating if the resulting quality of the fit improved substantially and if the uncertainty of the parameter was much smaller than a fifth of the magnitude of the parameter. Generally, we searched for the parameter whose fitting improved the quality most among the parameters reasonable to be fit. This procedure was repeated until the quality of the fit did not improve considerably anymore.

We evaluated initial spectroscopic parameters of $H_2C^{33}S$, $H_2C^{36}S$, and $H_2^{13}C^{34}S$ in a similar manner; the main difference was that we considered not only parameters of H_2CS, but also of $H_2C^{34}S$ and $H_2^{13}CS$. Nuclear HFS parameters had to be included in the fit of $H_2C^{33}S$. The dominant contribution comes from the nuclear electric quadrupole coupling. There are only three parameters, χ_{aa}, χ_{bb}, and χ_{cc}, because of the symmetry of the molecule; χ_{cc} was derived from the other two because the sum of the three is zero. Nuclear magnetic spin-rotation coupling parameters needed to be included in the fit also. However, the values of C_{bb} and C_{cc} were poorly determined and were quite different from values obtained from quantum-chemical calculations. It turned out that $C_{bb} - C_{cc}$ is well determined whereas $C_{bb} + C_{cc}$ appears to be insufficiently constrained. Therefore, we constrained $C_{bb} + C_{cc}$ to the value from an MP2 calculation because the remaining two experimental parameters agreed well with the calculated ones. Distortion parameters of HDCS and D_2CS that could not be evaluated experimentally were estimated from values taken from a quantum-chemical calculation (Martin et al. 1994) and considering deviations between these calculated equilibrium values and the determined experimental ground state values of these two isotopic species and those of H_2CS.

The spectroscopic parameters of H_2CS, $H_2C^{33}S$, $H_2C^{34}S$, and $H_2C^{36}S$ are given in Table 1, except for the $H_2C^{33}S$ hyperfine structure parameters which are presented in Table 2 in comparison to values from quantum-chemical calculations. The spectroscopic parameters of $H_2^{13}CS$, $H_2^{13}C^{34}S$, HDCS, and D_2CS are gathered in Table 3.

Table 4. Frequencies ν (GHz) and J values for which deviations between old calculations and present data exceed 1 MHz given for selected thioformaldehyde isotopic species and K_a values.

Isotopolog	K_a	ν	J
$H_2^{13}CS$	5	> 198.0	≥ 5
	2u[a]	> 330.5	≥ 9
	0	> 461.0	≥ 13
$H_2C^{34}S$	5	> 202.4	≥ 5
	4	> 269.9	≥ 7
	3	> 405.0	≥ 11
$H_2C^{33}S$	6	> 238.0	≥ 6
	5	> 306.1	≥ 8
	4	> 476.3	≥ 13

Notes. [(a)] Transitions with $K_c = J - 2$; transitions with $K_c = J - 1$ deviate less.

The experimental data have been reproduced within experimental uncertainties for all isotopic species. There is some scatter among partial data, e.g, previous rotational lines for a given isotopolog. Some partial data sets have been judged slightly conservatively.

The experimental transition frequencies with quantum numbers, uncertainties, and differences to the calculated frequencies in the final fits are available as supplementary material to this article. The line, parameter, and fit files along with auxiliary files are available in the data section of the CDMS.[3] Calculated and experimental transition frequencies for radio astronomical observations and other purposes are provided in the catalog section[4] of the CDMS.

Since Cox et al. (1982) determined the D_2CS dipole moment to be slightly larger than that of H_2CS, we discuss changes of dipole moments upon isotopic substitution. The experimentally determined difference between H_2CS and D_2CS is only 0.0105 ± 0.0011 D, equivalent to an overestimation of the D_2CS column density by about 1.3 %, which is negligible by astronomical standards. Fabricant et al. (1977) determined that the dipole moments of D_2CO is 0.0154 D larger than that of H_2CO whereas the one of D_2CCO is only 0.0024 D larger than the one of H_2CCO, suggesting that dipole moment differences upon deuteration decrease rapidly for increasingly larger molecules. Heavy atom substitution leads to much smaller differences. As may be expected, the dipole moment of $H_2^{13}CO$ is only 0.0002 D larger than that of H_2CO (Fabricant et al. 1977). Our ground state dipole moments, which we calculated at the B3LYP/QZ and MP2/QZ levels, yielded differences of similar magnitude upon heavy atom substitution. The difference in the case of D_2CS was 0.0136 D and 0.0132 D after scaling the values with the ratio between calculated H_2CS ground state dipole moment and the experimental value. These isotopic changes agree with the experimental one of Cox et al. (1982) within three times the uncertainty. Finally, we point out that the slight rotation of the inertial axis system in the case of HDCS leads to a minute b-dipole moment component of ~0.08 D. The strongest b-type transitions are around three orders of magnitude weaker than the strongest

[3] http://www.astro.uni-koeln.de/cdms/daten/H2CS

[4] website: http://www.astro.uni-koeln.de/cdms/entries/, see also http://www.astro.uni-koeln.de/cdms/catalog/

Table 5. Spectroscopic parameters[a] (MHz) of thioformaldehyde in comparison to those of related molecules.

Parameter	H_2CO[b]	H_2CS[c]	H_2SiO[d]	H_2SiS[e]
$A-(B+C)/2$	245551.4495 (40)	274437.5932 (115)	148946.49 (173)	162498.0 (14)
$(B+C)/2$	36419.11528 (25)	17175.745955 (196)	17711.07958 (33)	7844.48028 (22)
$(B-C)/4$	1207.4358721 (33)	261.6240523 (165)	483.74088 (50)	93.23731 (28)
D_K	19.39136 (53)	23.34378 (164)	7.63 (87)	9.811
D_{JK}	1.3211073 (93)	0.5222938 (43)	0.610532 (60)	0.151376 (44)
$D_J \times 10^3$	70.32050 (50)	19.01875 (39)	16.1803 (94)	3.92823 (27)
$d_1 \times 10^3$	−10.437877 (47)	−1.208429 (105)	−2.08116 (236)	−0.19581 (35)
$d_2 \times 10^3$	−2.501496 (33)	−0.1773270 (222)	−0.6712 (48)	−0.02938 (17)
$H_K \times 10^3$	4.027 (22)	5.946 (35)	1.0[f]	1.6[f]
$H_{KJ} \times 10^6$	10.865 (79)	−28.155 (86)	−43.324 (297)	−18.8 (15)
$H_{JK} \times 10^6$	7.465 (16)	1.50409 (270)	3.409 (65)	0.246 (34)
$H_J \times 10^9$	3.54 (33)	−5.81 (32)		
$h_1 \times 10^9$	32.272 (58)	3.018 (141)		
$h_2 \times 10^9$	47.942 (74)	1.6472 (140)		
$h_3 \times 10^9$	15.966 (15)	0.3619 (73)		
$L_K \times 10^6$	−0.610 (177)	−2.109 (206)		
$L_{KKJ} \times 10^9$	−5.85 (19)	−21.36 (69)		
$L_{JK} \times 10^9$	0.367 (85)	0.2032 (90)		
$L_{JJK} \times 10^{12}$	−105.7 (92)	−10.32 (81)		
$L_J \times 10^{12}$		0.833 (87)		
$l_1 \times 10^{12}$		−0.358 (47)		
$l_2 \times 10^{12}$	−0.345(50)			
$l_3 \times 10^{12}$	−0.427(19)			
$l_4 \times 10^{12}$	−0.1520 (32)			
$P_{KKJ} \times 10^{12}$		−18.63 (180)		
$p_5 \times 10^{18}$	3.33			

Notes. [a] Watson's S reduction has been used in the representation I^r. Numbers in parentheses are one standard deviation in units of the least significant figures. Parameters without uncertainties were estimated and kept fixed in the analyses. [b] Müller & Lewen (2017). [c] This work. [d] Bailleux et al. (1994); refit in the S reduction in the present work. [e] McCarthy et al. (2011) [f] Estimated in the present work.

a-type transitions at similar frequencies. Only the uncertainties of the $K_a = 1 \leftrightarrow 0$ transitions (~0.2 MHz) may be small enough to permit detection in astronomical spectra at least in theory. The uncertainties increase rapidly with increasing K_a.

Astronomers will be interested to know the impact of the present data on the calculated line positions. Deviations between initial calculations of transition frequencies and the present ones increase usually strongly with K_a and less strongly with J. We show in Table 4 for three isotopic species and selected values of K_a the J values and the corresponding frequencies for which these deviations exceed 1 MHz. This corresponds to the line width of the protostar IRAS 16293−2422 source B around 300 GHz; e.g., Drozdovskaya et al. (2018). Dark clouds may exhibit even smaller line widths, whereas high-mass star-forming regions usually display larger line widths by factors of a few.

Noticing that initially calculated and present transition frequencies of $H_2C^{34}S$ display differences of more than 1 MHz in the upper millimeter and lower submillimeter region for modest values of K_a, we wondered if the findings of Drozdovskaya et al. (2018) were affected by these differences. The paper is based on the Protostellar Interferometric Line Survey (PILS) of the binary IRAS 16293−2422 carried out with the Atacama Large Millimeter/submillimeter Array (ALMA) in the 329.15−362.90 GHz range (Jørgensen et al. 2016). The $J = 10 - 9$ transitions of $H_2C^{34}S$ are covered in that survey. The model by Drozdovskaya et al. (2018) shows that the $K_a = 3$ pair of transitions are near the noise limit, but are blended by stronger transitions. Shifts of almost 1 MHz between initially and presently calculated rest frequencies do not change this enough (Drosdovskaya, private communication to H.S.P.M., 2018). All but one of the remaining five transitions with lower K_a are clearly blended. Therefore, the finding by Drozdovskaya et al. (2018) that only an upper limit to the column density could be determined for $H_2C^{34}S$ remains unaltered.

We were able to determine $A - (B + C)/2$ for all isotopic species and for some even D_K although direct information on the purely K-dependent parameters exists only for the main species through the $\Delta K_a = 2$ rotational transitions and the ground state combination differences from Clouthier et al. (1994) and even though thioformaldehyde is so close to the symmetric prolate limit.

The experimental ^{33}S hyperfine structure parameters in Table 2 agree well or quite well with those from quantum-chemical calculations. We note that the calculated values are equilibrium values whereas the experimental ones are values referring to the ground vibrational state. Consideration of vibrational effects may have some influence on the comparison, but their evaluation was beyond the aim of our study.

A comparison of spectroscopic parameters of the isovalent molecules formaldehyde, thioformaldehyde, silanone, and

thiosilanone is given in Table 5. Interestingly, the quartic distortion parameters scale approximately with appropriate powers of $A - (B + C)/2$, $B + C$, and $B - C$. This appears to apply also for some of the available sextic distortion parameters, but in many cases the relations are more complex.

6. Structural parameters of thioformaldehyde

The equilibrium structure is the best and easiest defined structure of a molecule. It requires to calculate equilibrium rotational parameter(s), for example, B_e from the ground state rotational parameter(s) B_0 as follows

$$B_e = B_0 + \frac{1}{2}\sum_j \alpha_j^B - \frac{1}{4}\sum_{j\le k} \gamma_{jk}^B - ... \quad (1)$$

where the α_j^B are first order vibrational corrections, the γ_{jk}^B are second order vibrational corrections, and so on. Equivalent formulations hold for A_e and C_e. In the case of a diatomic molecule, only information on one isotopic species is necessary, and only one rotational parameter and one vibrational correction of each order exist. Experimental data exist for a plethora of diatomic molecules, see, e.g., Huber & Herzberg (1979). B_e is usually much larger than α which in turn is much larger than $|\gamma|$; the situation involving higher order corrections may be more complex.

The general n-atomic asymmetric rotor molecule has three different rotational parameters A, B, and C, $3n - 6$ first order vibrational corrections, $(3n - 6)(3n - 5)/2$ second order vibrational corrections, and so on. Specifically, the number of first and second order corrections are three and six, respectively, for a triatomic molecule, and six and 21 for a tetratomic molecule such as H_2CS. Experimental equilibrium structural parameters of polyatomic molecules with consideration of more than first order vibrational corrections are very rare, but more exist with consideration of first order vibrational corrections only. It is necessary to point out that $B_0 - B_j$ is only to first order equal to α_j^B. Moreover, data for more than one isotopic species are needed to determine all independent structural parameters unless the molecule is a symmetric triatomic of the type AB_2, where atoms A and B do not need to be different.

An alternative, lately very common, approach is to calculate $\sum_j \alpha_j^B$ by quantum-chemical means to derive semi-empirical equilibrium rotational parameters $B_{i,e}$ from the experimental ground state values (Stanton et al. 1998). Second and higher order vibrational contributions are neglected. Numerous quantum-chemical programs are available to carry out such calculations; examples have been mentioned in Sect. 3.

We have used B3LYP, MP2, and CCSD(T) calculations with an adequately large basis set of quadruple zeta quality to evaluate the first order vibrational corrections for isotopologs of thioformaldehyde which have been summarized in Table 6 together with ground state values, two additional corrections described in greater detail below, the final semi-empirical equilibrium values at the CCSD(T) level, and the corresponding equilibrium inertia defect Δ_e. The inertia defect is defined as $\Delta = I_{cc} - I_{bb} - I_{aa}$. Among the three methods employed in the present study, CCSD(T) is considered to be by far the most accurate one under most circumstances whereas MP2 and B3LYP are usually less accurate by different degrees. Morgan et al. (2018) performed extensive calculations on the related formaldehyde molecule. The ae-CCSD(T) data obtained with a basis set of QZ quality are already quite close to experimental values, but larger basis sets or higher degrees of electron correlation modify the picture somewhat. All corrections together improve the agreement between quantum-chemical calculations and experimental results non-negligibly. Such calculations are, however, very demanding, and in many cases ae-CCSD(T) calculations with a basis set of QZ quality are a good compromise for small to moderately large molecules (Coriani et al. 2005).

The $\Delta B_{i,\mathrm{v}}$ determined for thioformaldehyde differ considerably among the three methods for each isotopolog and each i. We suspect that the second order vibrational corrections are smaller than the differences between the methods. If we assume that they decrease in magnitude in a similar way as the first order corrections are smaller than the ground state rotational parameters, then the second order corrections to A should be around 10 MHz, and those to B and C should be less than 1 MHz.

Oka & Morino (1961) showed that the rotational Hamiltonian of a semirigid rotor contains two terms which cause the inertia defect Δ to be non-zero when the ground state rotational parameters $B_{i,0}$ were corrected for the vibrational corrections $\Delta B_{i,\mathrm{v}}$, namely an electronic contribution $\Delta B_{i,\mathrm{el}}$ and a centrifugal distortion contribution $\Delta B_{i,\mathrm{cent}}$. The electronic contribution is calculated as $\Delta B_{i,\mathrm{el}} = -B_{i,e}\, g_{ii}\, m_e/m_p$, where the g_{ii} are components of the rotational g-tensor and m_e and m_p are the masses of the electron and the proton, respectively (Oka & Morino 1961). We took the g_{ii} values of thioformaldehyde from the very accurate Zeeman measurements of Rock & Flygare (1972). The centrifugal distortion contribution is evaluated as $\Delta A_{\mathrm{cent}} = \Delta B_{\mathrm{cent}} = \hbar^4\, \tau_{abab}/2$ and $\Delta C_{\mathrm{cent}} = -3\hbar^4\, \tau_{abab}/4$ (Oka & Morino 1961). $\hbar^4\, \tau_{abab}$ ($= \tau'_{abab}$; tbc) is a distortion parameter which was evaluated here from an empirical force field calculated using the program NCA (Christen 1978).

The inertia defect Δ may be used an indication of the quality of the vibrational correction. The ground state value Δ_0 of the main isotopolog is 0.06139 amu Å^2, quite small and positive as can be expected for a small and rigid molecule. The equilibrium value should ideally be zero. However, the first order vibrational corrections lead usually to negative values which are much smaller in magnitude than the ground state values. In the case of our B3LYP, MP2, and CCSD(T) calculations, the values are −0.00381, −0.00305, and −0.00406 amu Å^2, respectively. Taking the electronic corrections into account, we obtain 0.00281, 0.00356, and 0.00255 amu Å^2, respectively, and finally, after applying the centrifugal distortion correction, 0.00020, 0.00093, and −0.000064 amu Å^2, respectively.

The equilibrium inertia defects in Table 6 show very small scatter very close to zero among five isotopic species, and slightly larger scatter for three others. Even though that larger scatter is still fairly small, it is worthwhile to look into potential sources for that finding. The smaller list of experimental lines could be an explanation for $H_2^{13}C^{34}S$ and for D_2CS, but not likely for HDCS. The Δ_e value of $H_2^{13}C^{34}S$ would be essentially zero if A_e were increased by 121 MHz. This can be ruled out safely because ideally A_e should not change upon substitution of one (or both) of the heavy atoms, and the $H_2^{13}C^{34}S$ value is only about 11 MHz larger than that of the main isotopolog albeit with an uncertainty of 16 MHz. A decrease of C_e by 0.35 MHz would also lead to $\Delta_e \approx 0$, but a corresponding change in the experimentally determined value of C_0 appears rather unlikely. We suspect that shortcomings in the CCDS(T) first order vibrational correction or the neglect of second order vibrational correction are mainly responsible for the somewhat larger scatter observed for three of the thioformaldehyde isotopologs, even more so, as

Table 6. Ground state rotational parameters $B_{g,0}$ of thioformaldehyde isotopic species, vibrational $\Delta B_{i,v}$[a], electronic $\Delta B_{i,el}$ and centrifugal corrections $\Delta B_{i,cent}$, coupled-cluster corrected semi-empirical equilibrium rotational parameters $B_{i,e}$(CCSD(T), and resulting equilibrium inertia defect Δ_e.[b]

Species	B_i	$B_{i,0}$	$\Delta B_{i,v}$(B3LYP)	$\Delta B_{i,v}$(MP2)	$\Delta B_{i,v}$(CCSD(T))	$\Delta B_{i,el}$	$\Delta B_{i,cent}$	$B_{i,e}$(CCSD(T)	Δ_e
H_2CS	*A*	291613.34	1671.810	1900.593	1958.684	843.435	−0.608	294414.850	
	B	17698.994	63.975	68.066	74.002	1.294	−0.608	17773.682	
	C	16652.498	98.197	102.170	108.190	0.218	0.912	16761.817	−0.000064
$H_2C^{33}S$	*A*	291612.9	1672.606	1901.179	1959.382	843.435	−0.598	294415.07	
	B	17538.843	63.279	67.354	73.212	1.282	−0.598	17612.739	
	C	16510.639	96.945	100.900	106.845	0.216	0.897	16618.596	−0.000049
$H_2C^{34}S$	*A*	291612.0	1673.333	1901.704	1960.038	843.435	−0.588	294414.91	
	B	17388.498	62.627	66.686	72.472	1.271	−0.588	17461.653	
	C	16377.325	95.774	99.712	105.586	0.215	0.882	16484.009	−0.000030
$H_2C^{36}S$	*A*	291609.7	1674.700	1902.681	1961.244	843.435	−0.571	294413.75	
	B	17111.828	61.430	65.458	71.122	1.251	−0.571	17183.630	
	C	16131.646	93.630	97.537	103.282	0.211	0.857	16235.996	0.000019
$H_2^{13}CS$	*A*	291628.8	1657.739	1884.781	1943.937	843.435	−0.567	294415.62	
	B	16998.786	59.621	63.806	69.345	1.243	−0.567	17068.807	
	C	16031.192	91.529	95.565	101.210	0.210	0.850	16133.462	0.000008
$H_2^{13}C^{34}S$	*A*	291638.	1658.041	1885.861	1944.755	843.435	−0.548	294426.	
	B	16685.867	57.814	61.982	67.761	1.220	−0.548	16754.300	
	C	15752.571	89.600	93.602	98.981	0.206	0.822	15852.580	−0.000705
HDCS	*A*	202715.3	930.335	1041.110	1070.464	585.478	−0.466	204370.79	
	B	16110.811	56.576	58.665	64.156	1.178	−0.466	16175.679	
	C	14891.548	88.063	90.525	95.721	0.195	0.699	14988.163	0.00255
D_2CS	*A*	146399.0	645.743	736.128	751.566	422.765	−0.369	147572.97	
	B	14904.267	50.835	51.155	56.344	1.089	−0.369	14961.330	
	C	13495.845	80.217	80.936	85.563	0.177	0.554	13582.139	0.00547

Notes. [(a)] $\Delta B_{i,v} = \sum_j \alpha_j^{B_i}$ calculated by different quantum-chemical means as detailed in Sect. 3. [(b)] All numbers in units of MHz, except Δ_e in units of amu Å^2.

the differences between the equilibrium inertia defects of H_2CS and $H_2^{13}C^{34}S$ are about twice as large if the CCDS(T) vibrational corrections are replaced by the B3LYP or MP2 corrections.

We employed the RU111J program (Rudolph 1995) to derive semi-empirical equilibrium structural parameters r_e^{SE} as well as $r_{I,\epsilon}$ parameters. The latter model was proposed by Rudolph (1991). The difference between ground state and equilibrium moments of inertia can be expressed as $I_{ii,0} = I_{ii,e} + \epsilon_i$, with $i = a, b, c$, assuming that the ϵ_i are equal among the different isotopologs of a given molecule. According to Rudolph (1991), the $r_{I,\epsilon}$ parameters are equivalent with $r_{\Delta I}$ parameters (isotopic differences are fit to determine structural parameters) and with substitution parameters r_s (isotopic differences between one reference isotopolog and one isotopolog in which one atom has been substituted are used to locate that atom). The advantage of considering the ϵ_i explicitely in the calculations are predictions of rotational parameters of isotopic species to be studied, see for example Epple & Rudolph (1992) and Müller & Gerry (1994). The resulting structural parameters are given in Table 7 together with earlier r_s parameters, ground state average (r_z) parameters and an approximation of the equilibrium structure derived from r_z parameters. The harmonic contributions to the ground state moments of inertia, obtained from a harmonic force field calculation, are subtracted off in the ground state average structure. The approximation of the equilibrium structure derived from r_z parameters assumes that anharmonic contributions to a given bond in a molecule can be approximated from the anharmonicity of the respective diatomic molecule, and differences in r_z and r_e bond angles are neglected (Turner et al. 1981). Table 7 also contains structural parameters of thioformaldehyde from several present and selected earlier quantum-chemical calculations.

The semi-empirical strutures r_e^{SE} determined with first order vibrational corrections obtained with three different methods are quite similar, albeit with some of the differences outside the combined uncertainties. The semi-empirical structure obtained with the CCSD(T) corrections is very close to the purely quantum-chemically derived ae-CCSD(T)/wQZ structure, as is very often the case (Coriani et al. 2005), and is probably closest to a purely experimental equilibrium structure. The CS bond lengths derived from B3LYP or MP2 calculations with basis sets of QZ quality are all too short, especially the ae-MP2 value. The CH bond lengths are all slightly too long, and the HCS bond angles all too large. The corresponding MP2 quantities are closer to our semi-empirical values.

Our $r_{I,\epsilon}$ parameters agree within combined uncertainties with the r_s parameters of Johnson et al. (1971), as is expected (Rudolph 1991), but less so with the r_s values of Cox et al. (1982). However, these latter r_s values are quite close to our r_e^{SE} values. The two sets of ground state average (r_z) parameters differ somewhat, but in both cases both bond lengths are longer

Table 7. Quantum-chemical and experimental bond lengths (pm) and bond angle (deg) of thioformaldehyde.[a]

Method[b]	r(CS)	r(CH)	∠(HCS)
B3LYP/TZ	160.614	108.786	122.202
B3LYP/QZ	160.516	108.711	122.208
B3LYP/awQZ	160.506	108.716	122.198
MP2/TZ	160.991	108.627	121.881
MP2/QZ	160.670	108.533	121.825
MP2/awCQZ	160.622	108.550	121.794
ae-MP2/awCQZ	160.188	108.390	121.767
CCSD(T)/TZ	161.826	108.766	121.928
CCSD(T)/QZ	161.415	108.683	121.841
ae-CCSD(T)/wCQZ	160.890	108.531	121.855
ae-CCSD(T)/wC5Z	160.797	108.512	121.815
CCSD(T)/QZ*[c]	160.90	108.53	121.77
dito, refined[d]	160.895	108.685	121.75
r_s[e]	161.08 (9)	109.25 (9)	121.57 (3)
r_s[f]	161.077 (1)	108.692 (3)	121.74 (2)
r_z[f]	161.38 (4)	109.62 (6)	121.87 (5)
r_z[g]	161.57 (8)	109.92 (21)	121.33 (29)
$r_e(r_z)$[g]	161.10 (8)	108.56 (21)	
$r_{I,\epsilon}$	161.025 (30)	109.246 (21)	121.562 (12)
$r_e^{\rm SE}$(B3LYP)	160.975 (2)	108.526 (6)	121.706 (5)
$r_e^{\rm SE}$(MP2)	160.934 (6)	108.556 (15)	121.759 (13)
$r_e^{\rm SE}$(CCSD(T))	160.909 (1)	108.531 (2)	121.758 (2)

Notes. [a] All values from this work unless indicated otherwise. Numbers in parentheses are one standard deviation in units of the least significant figures. [b] Quantum-chemical calculations as detailed in Sect. 3. [c] CCSD(T) calculation with basis sets up to QZ quality with extrapolation to infinite basis set size and with several corrections (Yachmenev et al. 2011). [d] Calculated rotational energies from Yachmenev et al. (2011) were adjusted to experimental energies by refining the structural parameters (Yachmenev et al. 2013). [e] Substitution structure r_s for H_2CS isotopolog from Johnson et al. (1971). [f] Substitution structure r_s and ground state average structure r_z for H_2CS isotopolog from Cox et al. (1982). [g] Ground state average structure r_z for H_2CS isotopolog and estimate of equilibrium bond lengths from r_z (Turner et al. 1981).

than the equilibrium values, as is usually the case. The equilibrium bond lengths derived from one of the r_z structures is in fairly good agreement with our $r_e^{\rm SE}$ values.

We recommend employment of first-order vibrational corrections obtained with the CCSD(T) method for semi-empirical structure determinations if high accuracy is desired. Less expensive methods may, however, be sufficient if accuracy requirements are less stringent.

7. Conclusion and outlook

We have obtained extensive sets of accurate transition frequencies for seven isotopic species of thioformaldehyde. They extend to beyond 900 GHz for $H_2C^{33}S$, for $H_2C^{36}S$, and for HDCS and even reach almost 1400 GHz in the cases of H_2CS, $H_2C^{34}S$, and $H_2^{13}CS$. The line list of the very rare $H_2^{13}C^{34}S$ extends to about 360 GHz. The resulting accurate spectroscopic parameters not only permit prediction of the strong R-branch transitions in the respective frequency range and up to K_a slightly beyond those covered in the line lists, but also permit reliable to reasonable extrapolation up to about twice the upper experimental frequencies and probably up to K_a covered in the line lists. Thus, accurate rest frequencies covering the entire present frequency range of ALMA are available for most thioformaldehyde isotopologs; in the case of $H_2^{13}C^{34}S$, they cover all bands up to band 9. In addition, the ^{33}S hyperfine structure of $H_2C^{33}S$ has been reevaluated based on previous and present data.

We carried out quantum-chemical calculations to evaluate first order vibrational corrections to the ground state rotational parameters in order to approximate equilibrium rotational parameters which lead to semi-empirical structural parameters. Quantum-chemical calculations were also carried out to obtain structural parameters directly.

Additional observed rest frequencies include, for example, data for excited vibrational states of H_2CS and $H_2C^{34}S$. We intend to report on these findings in a separate manuscript elsewhere in the near future.

Acknowledgements. We acknowledge support by the Deutsche Forschungsgemeinschaft via the collaborative research centers SFB 494 (project E2) and SFB 956 (project B3) as well as the Gerätezentrum SCHL 341/15-1 ("Cologne Center for Terahertz Spectroscopy"). We are grateful to NASA for its support of the OSU program in laboratory astrophysics and the ARO for its support of the study of large molecules. HSPM thanks C. P. Endres and M. Koerber for support during some of the measurements in Köln. Our research benefited from NASA's Astrophysics Data System (ADS).

References

Agúndez, M., Fonfría, J. P., Cernicharo, J., Pardo, J. R., & Guélin, M. 2008, A&A, 479, 493

Bailleux, S., Bogey, M., Demuynck, C., Destombes, J.-L., & Walters, A. 1994, J. Chem. Phys., 101, 2729

Becke, A. D. 1993, J. Chem. Phys., 98, 5648

Beers, Y., Klein, G. P., Kirchhoff, W. H., & Johnson, D. R. 1972, J. Mol. Spectrosc., 44, 553

Belov, S. P., Lewen, F., Klaus, T., & Winnewisser, G. 1995, J. Mol. Spectrosc., 174, 606
Berglund, M., & Wieser, M. E. 2011, Pure Appl. Chem., 83, 397
Brown, R. D., Godfrey, P. D., McNaughton, D., & Yamanouchi, K. 1987, Mol. Phys., 62, 1429
Christen, D. 1978, J. Mol. Struct., 48, 101
Clouthier, D. J., Huang, G., Adam, A. G., & Merer, A. J. 1994, J. Chem. Phys., 101, 7300
Coriani, S., Marchesan, D., Gauss, J., et al. 2005, J. Chem. Phys., 123, 184107
Cox, A. P., Hubbard, S. D., & Kato, H. 1982, J. Mol. Spectrosc., 93, 196
Crockett, N. R., Bergin, E. A., Neill, J. L., et al. 2014, ApJ, 787, 112
Cummins, S. E., Linke, R. A., & Thaddeus, P. 1986, ApJS, 60, 819
De Lucia, F. C. 2010, J. Mol. Spectrosc., 261, 1
Drozdovskaya, M. N., van Dishoeck, E. F., Jørgensen, J. K., et al. 2018, MNRAS, 476, 4949
Dubernet, M. L., Boudon, V., Culhane, J. L., et al. 2010, J. Quant. Spectrosc. Radiat. Transfer, 111, 2151
Dubernet, M. L., Antony, B. K., Ba, Y. A., et al. 2016, J. Phys. B, 49, 074003
Dunning, T. H., Jr. 1989, J. Chem. Phys., 90, 1007
Dunning, T. H., Jr., Peterson, K. A., & Wilson, A. K. 2001, J. Chem. Phys., 114, 9244
Endres, C. P., Schlemmer, S., Schilke, P., Stutzki, J., & Müller, H. S. P. 2016, J. Mol. Spectrosc., 327, 95
Epple, K. J. & Rudolph, H. D. 1992, J. Mol. Spectrosc., 152, 355
Fabricant, B., Krieger, D., & Muenter, J. S. 1977, J. Chem. Phys., 67, 1576
Gaussian 09, Revision E.01, Frisch, M. J., Trucks, G. W., Schlegel, H. B., et al., Gaussian, Inc., Wallingford CT, 2013.
Gardner, F. F., Hoglund, B., Shukre, C., Stark, A. A., & Wilson, T. L. 1985, A&A, 146, 303
Groner, P., Winnewisser, M., Medvedev, I. R., et al. 2007, ApJS, 169, 28
Heikkilä, A., Johansson, L. E. B., & Olofsson, H. 1999, A&A, 344, 817
Huber, K. P. & Herzberg, G. Molecular Spectra and Molecular Structure: IV. Constants of Diatomic Molecules. 1979, Van Nostrand Reinhold, New York
Irvine, W. M., Friberg, P., Kaifu, N., et al. 1989, ApJ, 342, 871
Johnson, D. R., & Powell, F. X. 1970, Science, 169, 679
Johnson, D. R., Powell, F. X., & Kirchhoff, W. H. 1971, J. Mol. Spectrosc., 39, 136
Jørgensen, J. K., van der Wiel, M. H. D., Coutens, A., et al. 2016, A&A, 595, A117
Lee, C., Yang, W., & Parr, R. G. 1988, Phys. Rev. B, 37, 785
Maeda, A., De Lucia, F. C., Herbst, E., et al. 2006, ApJS, 162, 428
Maeda, A., Medvedev, I. R., Winnewisser, M., et al. 2008, ApJS, 176, 543
Marcelino, N., Cernicharo, J., Roueff, E., Gerin, M., & Mauersberger, R. 2005, ApJ, 620, 308
Martin, J. M. L., Francois, J. P., & Gijbels, R. 1994, J. Mol. Spectrosc., 168, 363
Martín, S., Martín-Pintado, J., Mauersberger, R., Henkel, C., & García-Burillo, S. 2005, ApJ, 620, 210
McCarthy, M. C., Gottlieb, C. A., Thaddeus, P., Thorwirth, S., & Gauss, J. 2011, J. Chem. Phys., 134, 034306
McNaughton, D., & Bruget, D. N. 1993, J. Mol. Spectrosc., 159, 340
Medvedev, I., Winnewisser, M., De Lucia, F. C., et al. 2004, J. Mol. Spectrosc., 228, 314
Medvedev, I. R., Winnewisser, M., Winnewisser, B. P., De Lucia, F. C., & Herbst, E. 2005, J. Mol. Struct., 742, 229
Mills, I. M., "Vibration-Rotation Structure in Asymmetric- and Symmetric-Top Molecules", in "Modern Spectroscopy: Modern Research", Rao, K. N. & Matthews, C. W., eds., Academic Press, New York, NY, USA, vol. I, 1972; pp. 115−140
Minowa, H., Satake, M., Hirota, T., et al. 1997, ApJ, 491, L63
Møller, C. & Plesset, M. S. 1934, Phys. Rev., 46, 618
Morgan, W. J., Matthews, D. A., Ringholm, M., et al. 2018, J. Chem. Theory Comput., 14, 1333
Muller, S., Beelen, A., Guélin, M., et al. 2011, A&A, 535, A103
Müller, H. S. P., & Gerry, M. C. L. 1994, J. Chem. Soc. Faraday Trans., 90, 2601
Müller, H. S. P., & Brünken, S. 2005, J. Mol. Spectrosc., 232, 213
Müller, H. S. P., & Lewen, F. 2017, J. Mol. Spectrosc., 331, 28
Müller, H. S. P., McCarthy, M. C., Bizzocchi, L., et al. 2007, Phys. Chem. Chem. Phys., 9, 1579
Müller, H. S. P., Brown, L. R., Drouin, B. J., et al. 2015, J. Mol. Spectrosc., 312, 22
Müller, H. S. P., Drouin, B. J., Pearson, J. C., et al. 2016, A&A, 586, A17
Neill, J. L., Bergin, E. A., Lis, D. C., et al. 2014, ApJ, 789, 8
Oka, T., & Morino, Y. 1961, J. Mol. Spectrosc., 6, 472
Olofsson, A. O. H., Persson, C. M., Koning, N., et al. 2007, A&A, 476, 791
Persson, C. M., Olofsson, A. O. H., Koning, N., et al. 2007, A&A, 476, 807
Peterson, K. E. & Dunning, T. H., Jr. 2002, J. Chem. Phys., 117, 10548
Petkie, D. T., Goyette, T. M., Bettens, R. P. A., et al. 1997, Rev. Sci. Instrum., 68, 1675
Pickett, H. M. 1991, J. Mol. Spectrosc., 148, 371
Raghavachari, K., Trucks, G. W., Pople, J. A. & Head-Gordon, M. 1989, Chem. Phys. Lett., 157, 479
Rock, S. L., & Flygare, W. H. 1972, J. Chem. Phys., 56, 4723
Rudolph, H. D. 1991, Struct. Chem, 2, 581
Rudolph, H. D., "Accurate Molecular Structure from Microwave Rotational Spectroscopy", in "Advances in Molecular Structure Research", Hargittai, I. & Hargittai, M., eds., JAI Press Inc., Greenwich, CT, USA, vol. I, 1995
Schilke, P., Groesbeck, T. D., Blake, G. A., Phillips, & T. G. 1997, ApJS, 108, 301
Schilke, P., Benford, D. J., Hunter, T. R., Lis, D. C., & Phillips, T. G. 2001, ApJS, 132, 281
Sinclair, M. W., Fourikis, N., Ribes, J. C., et al. 1973, Aust. J. Phys., 26, 85
Stanton, J. F., Lopreore, C. L., & Gauss, J. 1998, J. Chem. Phys., 108, 7190
Turner, P. H., Halonen, L., & Mills, I. M. 1981, J. Mol. Spectrosc., 88, 402
Winnewisser, G., Krupnov, A. F., Tretyakov, M. Y., et al. 1994, J. Mol. Spectrosc., 165, 294
Winnewisser, G. 1995, Vib. Spectrosc., 8, 241.
Woodney, L. M., A'Hearn, M. F., McMullin, J., & Samarasinha, N. 1997, Earth Moon and Planets, 78, 69
Xu, L.-H., Lees, R. M., Crabbe, G. T., et al. 2012, J. Chem. Phys., 137, 104313
Yachmenev, A., Yurchenko, S. N., Ribeyre, T., & Thiel, W. 2011, J. Chem. Phys., 135, 074302
Yachmenev, A., Polyak, I., & Thiel, W. 2013, J. Chem. Phys., 139, 204308

Appendix A. Supplementary material

Table 8. Assigned transitions for the $H_2C^{34}S$ isotopic species as an example, observed transition frequencies (MHz)[a], experimental uncertainties Unc. (MHz)[a], residual O−C between observed frequencies and those calculated from the final set of spectroscopic parameters (MHz)[a], weight for blended lines, and sources of lines.

J'	K'_a	K'_c	$F'+0.5$	J''	K''_a	K''_c	$F''+0.5$	Frequency	Unc.	O−C	Weight	Source
6	1	5		6	1	6		21230.15	0.05	−0.01256		Cox et al. (1982)
7	1	6		7	1	7		28304.63	0.05	0.01393		Cox et al. (1982)
1	0	1		0	0	0		33765.80	0.05	0.05051		Cox et al. (1982)
8	1	7		8	1	8		36388.01	0.05	−0.07933		Cox et al. (1982)
2	1	2		1	1	1		66517.88	0.10	−0.02248		Johnson et al. (1971)
2	0	2		1	0	1		67528.15	0.10	−0.11515		Johnson et al. (1971)
2	1	1		1	1	0		68539.94	0.16	−0.23319		Johnson et al. (1971)
15	1	14		15	1	15		121120.1500	0.100	−0.03361		OSU
4	1	4		3	1	3		133026.9097	0.050	−0.01021		OSU
4	3	2		3	3	1		135027.8171	0.050	0.01347	0.5000	OSU
4	3	1		3	3	0		135027.8171	0.050	0.01347	0.5000	OSU
4	0	4		3	0	3		135030.6546	0.050	−0.00998		OSU
41	6	36		40	6	35		1378757.4655	0.010	−0.00721	0.5000	Koeln
41	6	35		40	6	34		1378757.4655	0.010	−0.00721	0.5000	Koeln
41	4	38		40	4	37		1380675.2953	0.010	0.00481		Koeln
41	4	37		40	4	36		1380920.5593	0.010	0.00223		Koeln
41	3	39		40	3	38		1380944.1970	0.010	−0.00340		Koeln
42	1	42		41	1	41		1385516.6458	0.010	−0.02038		Koeln

Notes. This table as well as those of other isotopologs are available in their entirety in the electronic edition in the online journal: http://cdsarc.ustrasbg.fr/cgi-bin/VizieR?-source=J/A+A/Vol/Num. A portion is shown here for guidance regarding its form and content. The F quantum numbers are redundant for all species except for $H_2C^{33}S$. [(a)] Negative uncertainties in the line list of the main isotopic species signal that units are cm^{-1} instead of MHz.